Defence Research and Development Canada
Recherche et développement pour la défense Canada

DEFENCE R&D DÉFENSE

Application of Joint Time-Frequency Representations to a Maneuvering Air Target in Sea-Clutter: Analysis Beyond FFT

T. Thayaparan and S. Kennedy

Defence R&D Canada – Ottawa
TECHNICAL MEMORANDUM
DRDC Ottawa TM 2003-090
March 2003

Canada

Application of Joint Time-Frequency Representations to a Maneuvering Air Target in sea-clutter: analysis beyond FFT

T. Thayaparan
Defence R&D Canada - Ottawa

S. Kennedy
Carleton University

Defence R&D Canada - Ottawa

Technical Memorandom

DRDC Ottawa TM 2003-090

March 2003

Abstract

Traditionally, radar signals have been analysed in either the time or the frequency domain. Joint time-frequency representations characterize signals over a time-frequency plane. They thus combine time-domain and frequency-domain analyses to yield a potentially more revealing picture of the temporal localization of a signal's spectral components. Therefore, for air target returns with time-varying frequency content, the joint time-frequency representations offer a powerful analysis tool. A concise review of time-frequency transforms is provided as background and is needed to appreciate how time-frequency processing methods can improve conventional time or frequency processing methods. The report then describes and illustrates the advantages of using joint time-frequency techniques to analyze a multi-component signal, a noisy signal, and experimental aircraft data. Finally, we use time-frequency analysis techniques for the detection of maneuvering aircraft using HF radar in heavily cluttered regions. We compare the ability of different time-frequency transforms to resolve several experimental aircraft returns. The results clearly demonstrate that time-frequency analysis techniques can significantly improve the detection performance of the HF radar and add considerable physical insight over what can be achieved by conventional Fourier transform methods currently used by HF radars.

Résumé

Par le passé, les signaux radar ont été analysés soit dans le domaine temporel, soit dans le domaine fréquentiel. Les représentations temps-fréquence mixtes montrent les caractéristiques des signaux sur un plan temps-fréquence. Elles combinent ainsi les analyses du domaine temporel et du domaine fréquentiel pour donner une image potentiellement plus révélatrice de l'emplacement temporel des composantes spectrales d'un signal. Par conséquent, les représentations temps-fréquence mixtes constituent un outil d'analyse puissant des signaux dont le contenu fréquentiel varie dans le temps. Nous présentons une brève étude des transformations temps-fréquence afin de fournir la base nécessaire pour apprécier la façon dont les méthodes de traitement temps-fréquence permettent d'améliorer les méthodes classiques de traitement temporel ou fréquentiel. Ensuite, le rapport décrit et illustre les avantages de l'utilisation des techniques temps-fréquence mixtes pour l'analyse d'un signal à plusieurs composantes, d'un signal perturbé par le bruit et de données expérimentales d'aéronef. Enfin, nous utilisons les techniques d'analyse temps-fréquence pour la détection d'un aéronef effectuant des manœuvres en ayant recours au radar HF dans des zones à niveau de clutter élevé. Nous comparons la capacité de différentes transformations temps-fréquence pour résoudre plusieurs signaux expérimentaux d'aéronef. Les résultats montrent clairement que les techniques d'analyse temps-fréquence permettent d'améliorer de façon appréciable l'efficacité de détection du radar HF et d'acquérir beaucoup d'autres connaissances physiques par comparaison aux méthodes à transformation de Fourier classiques qui sont actuellement utilisées par les radars HF.

Executive summary

One of the central problems in exploiting High Frequency (HF) radar data is the analysis of a time series. The problem at hand is how to extract the information present in the data and use it to its full potential. In order to address this problem we turn to the field of signal analysis and data representations. Traditionally, radar signals have been analysed in either the time or the frequency domain. The Fourier Transform is at the heart of a wide range of techniques that are used in HF radar data analysis and processing. Mapping the data into the temporal frequency domain is an effective way of recording the data such that their global characteristics can be assessed. However, the change of frequency content with time is one of the main features we observe in HF radar data. Because of this change of frequency content with time, radar signals belong to the class of non-stationary signals. The analysis of non-stationary signals requires technique that extend the notion of a global frequency spectrum to a local frequency description. The spectral energy density function that is obtained by means of a Fourier Transform, the so-called power spectrum, shows the frequencies that are present in our data, but does not reveal where changes in the frequency content occur. Consequently, for the interpretation of radar data in terms of a changing frequency content, we need a representation of our data as a function of both time and frequency. Only, quite recently, the joint time-frequency representation of signals has become a major area of research in radar signal processing.

The time-frequency representations characterize signals over a time-frequency plane. They thus combine time-domain and frequency-domain analyses to yield a potentially more revealing picture of the temporal localization of a signal's spectral components. They may also serve as a basis for signal detection, imaging, characterization, coding, and processing. A complete and comprehensive theory for joint time-frequency analysis does not yet exist. There is no unique time-frequency representation of a signal that satisfies all the properties of a physically correct joint time-frequency energy density function. However, discarding the requirement that all properties must be satisfied in one time-frequency representation, a class of joint time-frequency representations can be derived that serves as a model of a local power spectrum.

In this report, a concise review of time-frequency transforms is provided as background and is needed to appreciate how time-frequency processing methods can improve conventional time or frequency processing methods. The report then describes and illustrates the advantages of using joint time-frequency techniques to analyze a multi-component signal, a noisy signal, and experimental aircraft data. Finally, we use time-frequency analysis techniques for the detection of maneuvering aircraft using HF radar in heavily cluttered regions. We compare the ability of different time-frequency transforms to resolve several experimental aircraft signals. The results clearly demonstrate that time-frequency analysis techniques can significantly improve the detection performance of the HF radar and add considerable physical insight over what can be achieved by conventional Fourier transform methods currently used by HF radars.

T. Thayaparan , S. Kennedy. 2003. Application of Joint Time-Frequency Representations to a Maneuvering Air Target in sea-clutter: analysis beyond FFT. DRDC Ottawa TM 2003-090. Defence R&D Canada - Ottawa.

Sommaire

L'analyse d'une série chronologique constitue l'un des principaux problèmes éprouvés avec les données du radar haute fréquence (HF). Le problème qui se pose consiste à trouver un moyen pour extraire l'information contenue dans les données et pour l'utiliser à son plein potentiel. Pour résoudre ce problème, nous faisons appel au domaine de l'analyse des signaux et de la représentation des données. Par le passé, les signaux radar ont été analysés soit dans le domaine temporel, soit dans le domaine fréquentiel. La transformation de Fourier est au cœur d'une vaste gamme de techniques qui sont utilisées pour l'analyse et le traitement des données du radar HF. La mise en correspondance des données dans le domaine des fréquences temporelles constitue un moyen efficace pour enregistrer les données de telle façon que leurs caractéristiques globales puissent être évaluées. Cependant, la variation du contenu fréquentiel avec le temps est une des principales caractéristiques que nous observons dans les données du radar HF. En raison de cette variation du contenu fréquentiel avec le temps, les signaux radar appartiennent à la catégorie des signaux non stationnaires. Pour l'analyse des signaux non stationnaires, il faut avoir recours à des techniques qui élargissent la notion d'un spectre de fréquences global à une description de fréquence locale. La fonction de densité d'énergie spectrale obtenue au moyen d'une transformation de Fourier, et appelée le spectre de puissance, montre quelles fréquences sont contenues dans nos données, mais n'indique pas où se produisent les changements du contenu fréquentiel. Par conséquent, pour l'interprétation des données radar du point de vue d'un contenu fréquentiel changeant, nous avons besoin d'une représentation de nos données en fonction du temps et de la fréquence. Ce n'est que tout récemment que la représentation temps-fréquence mixte des signaux est devenue un sujet important de recherche dans le traitement des signaux radar.

Les représentations temps-fréquence mixtes montrent les caractéristiques des signaux sur un plan temps-fréquence. Elles combinent ainsi les analyses du domaine temporel et du domaine fréquentiel pour donner une image potentiellement plus révélatrice de l'emplacement temporel des composantes spectrales d'un signal. Elles peuvent aussi servir de base pour la détection des signaux, l'imagerie, la caractérisation, le codage et le traitement. Il n'existe pas encore de théorie complète et détaillée pour l'analyse temps-fréquence mixte. Il n'existe pas de représentation temps-fréquence unique d'un signal qui satisfait à toutes les propriétés d'une fonction de densité d'énergie temps-fréquence mixte correcte du point de vue physique. Cependant, si on fait abstraction de l'exigence selon laquelle il faut satisfaire à toutes les propriétés dans une seule représentation temps-fréquence, on peut établir une classe de représentations temps-fréquence mixtes qui sert de modèle pour un spectre de puissance local.

Dans ce rapport, nous présentons une brève étude des transformations temps-fréquence afin de fournir la base nécessaire pour apprécier la façon dont les méthodes de traitement temps-fréquence permettent d'améliorer les méthodes classiques de traitement temporel ou fréquentiel. Ensuite, le rapport décrit et illustre les avantages de l'utilisation des techniques temps-fréquence mixtes pour l'analyse d'un signal à

plusieurs composantes, d'un signal perturbé par le bruit et de données expérimentales d'aéronef. Enfin, nous utilisons les techniques d'analyse temps-fréquence pour la détection d'un aéronef effectuant des manœuvres en ayant recours au radar HF dans des zones à niveau de clutter élevé. Nous comparons la capacité de différentes transformations temps-fréquence pour résoudre plusieurs signaux expérimentaux d'aéronef. Les résultats montrent clairement que les techniques d'analyse temps-fréquence permettent d'améliorer de façon appréciable l'efficacité de détection du radar HF et d'acquérir beaucoup d'autres connaissances physiques par comparaison aux méthodes à transformation de Fourier classiques qui sont actuellement utilisées par les radars HF.

T. Thayaparan , S. Kennedy. 2003. Application of Joint Time-Frequency Representations to a Maneuvering Air Target in sea-clutter: analysis beyond FFT. DRDC Ottawa TM 2003-090. R & D pour la defénse Canada - Ottawa.

Table of contents

List of figures

This page intentionally left blank.

1. Introduction

One fundamental mathematical tool employed in radar signal processing is a transform. When asked to multiply the Roman numerals LXIV and XXXII, only a few of us will be able to give the correct answer right away. However, if the Roman numerals are first translated into Arabic numerals, 64 and 32, then all of us can get 2048 immediately. The process of converting the unfamiliar Roman numerals into common Arabic numerals is a typical example of transforms [1]. By properly applying transforms, we can simplify calculations or make certain attributes of the signal explicit.

One of the most popular transforms known to scientists and engineers is the Fourier transform that converts a signal from the time-domain to the frequency-domain. In fact, the Fourier transform is not simply a mathematical tool to make calculations easier. It also acts as a mathematical prism to break down a signal into a group of waveforms (different frequencies), as a prism breaks up light into a color spectrum. The Fourier transform is so powerful that people tend to apply it everywhere without noticing one fundamental difference between the mathematical prism and a real prism. The spectrum produced by the prism in the morning is different from that in the evening. We may say that the prism gives instantaneous spectra. Using a prism to examine spectra of light, there is no need for the information about light that existed million years ago and the light that will be there tomorrow. However, this is not the case for Fourier transform. To compute the Fourier transform, we not only need previous information, but also information that have not yet occurred. The spectrum computed by the Fourier transform is the spectrum averaged over an infinitely long time before the present to an infinitely long time after the present! [2]

The time series signals of radar targets have been traditionally analyzed in the frequency-domain. The transformation of a time series into a frequency-domain using the Fourier transform provides useful information regarding the target. However, Fourier spectral analysis is not without its shortcomings. The most prominent shortcoming of Fourier spectral analysis is its inability to properly represent frequency contents that changes over an observation period. *'The most widely used signal processing tool is the FFT (fast Fourier transform); the most widely misused signal processing tool is also the FFT"* [2]. Fourier transform-based techniques are effective as long as the frequency contents of the signal do not change with time. However, when the frequency contents of the data samples evolve over an observation period, other alternative methods should be considered. Joint time-frequency representations were developed to overcome this limitation of Fourier spectral analysis [3-4].

The joint time-frequency analysis has been a topic of much interest in the signal processing community in the past decade . Over the past ten years, radar researchers have also investigated time-frequency transforms as a unique tool for radar-specific signal analysis and image processing applications [2,5-9]. Both traditional time-frequency techniques, as well as the new tools developed in the signal processing community, have been applied to various radar problems. Like the developments in

other fields, such as underwater acoustics and speech processing, it was found that time-frequency transforms provide additional insight into the analysis, interpretation, and processing of radar signals that is sometimes superior to what is achievable in the traditional time or frequency domain alone. The specific applications where time-frequency transforms have been used include signal analysis and feature extraction, motion compensation and image formation, signal denoising, imaging of moving targets, and detection of moving targets [2,5-9].

Joint time-frequency representations transform a one-dimensional time signal into two-dimensional representation in the time-frequency plane. In this representation, time varying frequency can be easily displayed and studied. An important advantage of time-frequency representations is the ease of identifying target signals. A waveform with multiple signals or noise can become too complicated for visual analysis of its waveform. Even the Fourier spectral analysis can become garbled beyond recognition. Since time-frequency representations display time-varying frequencies, the signals are distinguishable from the noise. The nature of each signal can be easily seen.

This report demonstrates the usefulness and effectiveness of time-frequency representations and compares various time-frequency transforms. Three cases are examined to show the usefulness of time-frequency representations. The first case involves chirp signals that cannot be identified using Fourier spectral analysis. The second case involves a signal with noise. The data in these cases are simulated with complex values to be similar to real data. The third case shows the overall effectiveness of time-frequency representations in signal analysis. This case uses real aircraft data.

There are many different time-frequency representations available in the literature for analysis [2,5-10]. Each transform offers advantages and disadvantages. Certain transforms provide excellent resolution, but are slow to calculate. Others provide poor resolution, but are quick to calculate. Some transforms provide a good balance of speed and resolution, but have interference cross-terms. Although there are many different transforms available, we compare the ability of only twelve transforms to resolve several real aircraft signals. The main objective of this report is to demonstrate the effectiveness of time-frequency transforms for detecting maneuvering air targets in heavily cluttered environment. Twelve transforms that are considered for comparison and evaluation are the adaptive energy distribution, Born-Jordan distribution, binomial distribution, Choi-Williams distribution, Gabor representation, Margenau-Hill spectrogram, smoothed Wigner-Ville distribution, spectrogram distribution, Zhao-Atlas-Marks distribution, reassigned Gabor representation, reassigned Morlet scalogram, and the reassigned spectrogram distribution. Other time-frequency transforms that are available in the literature will be evaluated and compared in a future report. These twelve transforms are compared with experimental radar data. There are several examples of target returns with varying behavior to test the transforms in different situations. Each transform is then evaluated individually and against the group.

2. Advantages of Time-Frequency Representations

Time-frequency representations can drastically simplify the interpretation of signals. These representations provide a much clearer image of the signals due to their ability to display frequency that changes over time. To show this advantage more clearly, we will examine three cases. The first case consists of multiple chirp signals. The second case consists of a signal present in noise. These cases use simulated data with complex values. The third case uses experimental aircraft data to show the usefulness of time-frequency representations for signal analysis.

2.1 Detecting Multiple Signals

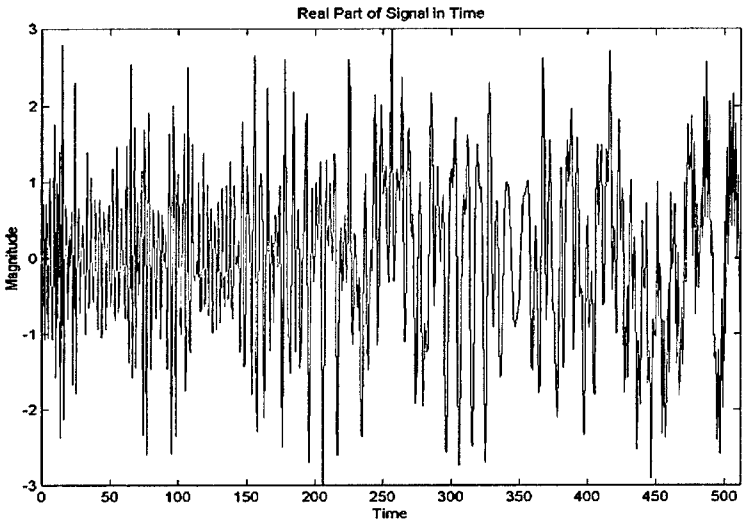

Figure 1: *Time series of multi-component signal*

There are multiple chirps present in the signal whose time series is displayed in Figure 1. The spectrum of the signal can be found using the Fourier transform. The signal as it appears in the frequency-domain is displayed in Figure 2. From the spectrum, it is difficult to identify the number of signals, and extremely difficult to determine their nature. Only an experienced signal analyzer may be able to determine these. A time-frequency representation makes signal analysis almost instantaneous. The Margenau-Hill spectrogram (see Section 3.2) of the signal is displayed in Figure 3. From the time-frequency representation it is immediately evident that there are three chirp signals. The nature of the chirps is easily determined as well. All three chirps have linear frequency modulation. Two chirps have decreasing frequency, one from 0.45 to 0.05 Hz and the other from 0.35 to -0.05 Hz. The third chirp has increasing frequency from –0.5 to 0.5 Hz. The time-frequency representation can easily be interpreted by someone with little signal analyzing experience.

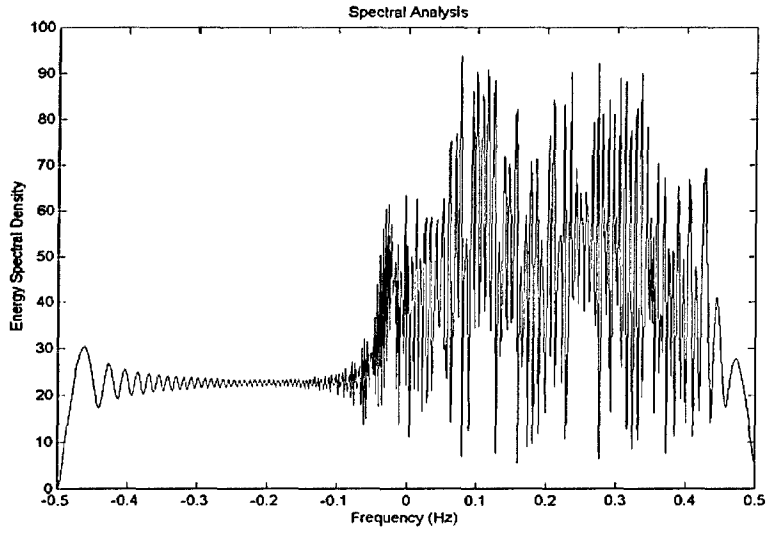

Figure 2: *The spectrum of the multi-component signal*

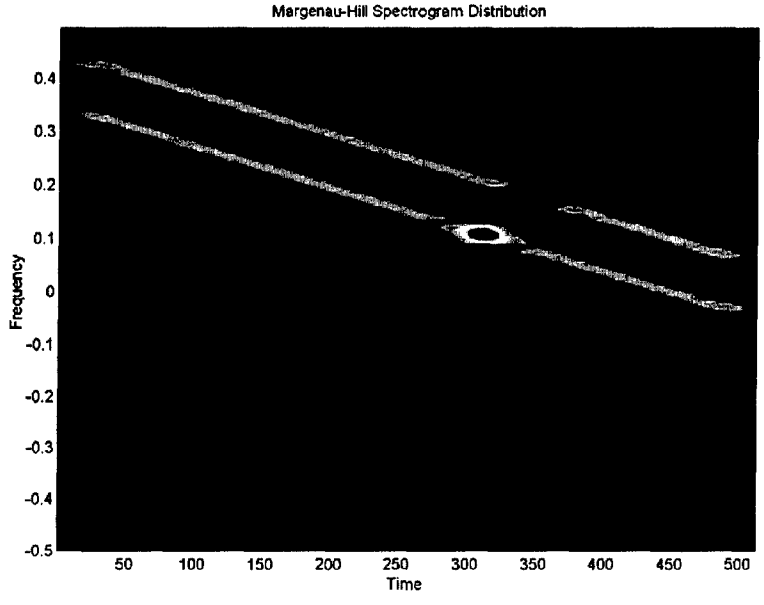

Figure 3: *The Margenau-Hill spectrogram of the multi-component signal*

2.2 Extracting a Signal from Noise

Due to the non-ideal conditions in collecting real data, signals will usually be noisy. Detecting the signal through the noise is a very important procedure. Figure 4 shows a signal hidden among complex white Gaussian noise. The signal was created by adding noise to a generated chirp signal.

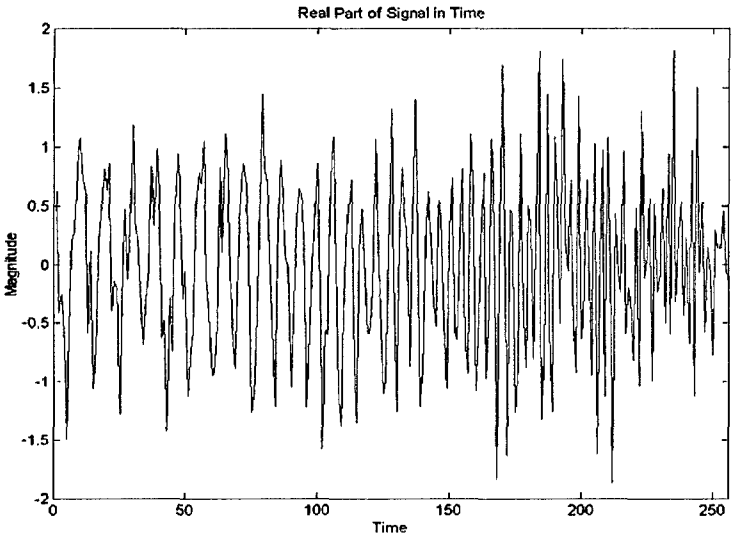

Figure 4: *Time series of a signal in white Gaussian noise*

From the time series it is difficult to detect the signal and nearly impossible to determine its nature. The spectrum of the signal, shown in Figure 5, is difficult to read. The target signal is indistinguishable from the noise.

Looking at a time-frequency representation of the signal in noise, it is clear that the signal is a single chirp. In Figure 6, the signal can be seen arching across the time-frequency plane. The spectrum of the signal does not provide an accurate method of analyzing the signal. In order to properly identify the noisy target signal, a time-frequency representation is needed.

Once the signal is identified, the noise can be filtered out. In this case, the transform is run through a high pass filter. The filtered signal can then be time-averaged to convert the signal to its one-dimensional frequency-domain representation. To convert this frequency-domain signal back to the time-domain, the inverse Fourier transform is taken. The filtered time-frequency representation and the recovered signal are shown in Figure 7. The recovered signal is black and the original signal before noise was added is grey. Using more accurately matched filters will increase the quality of the recovered signal.

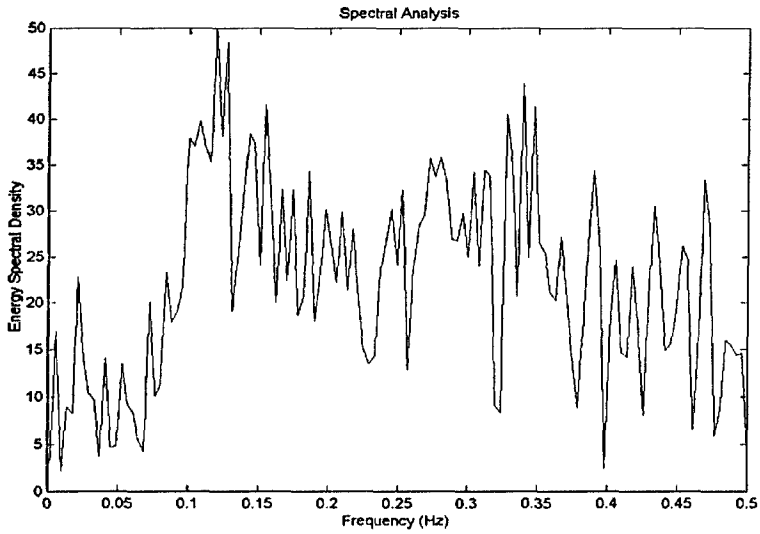

Figure 5: *The spectrum of a signal in white Gaussian noise*

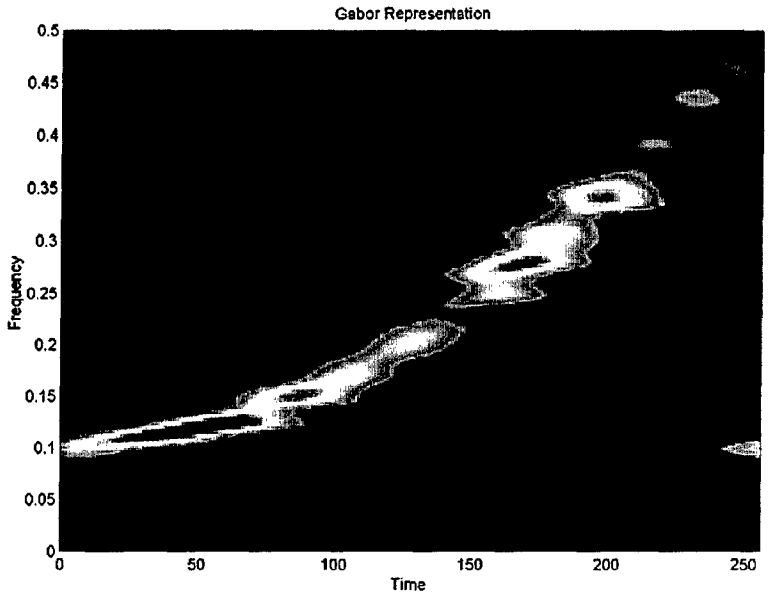

Figure 6: *A time-frequency representation of a signal in white Gaussian noise*

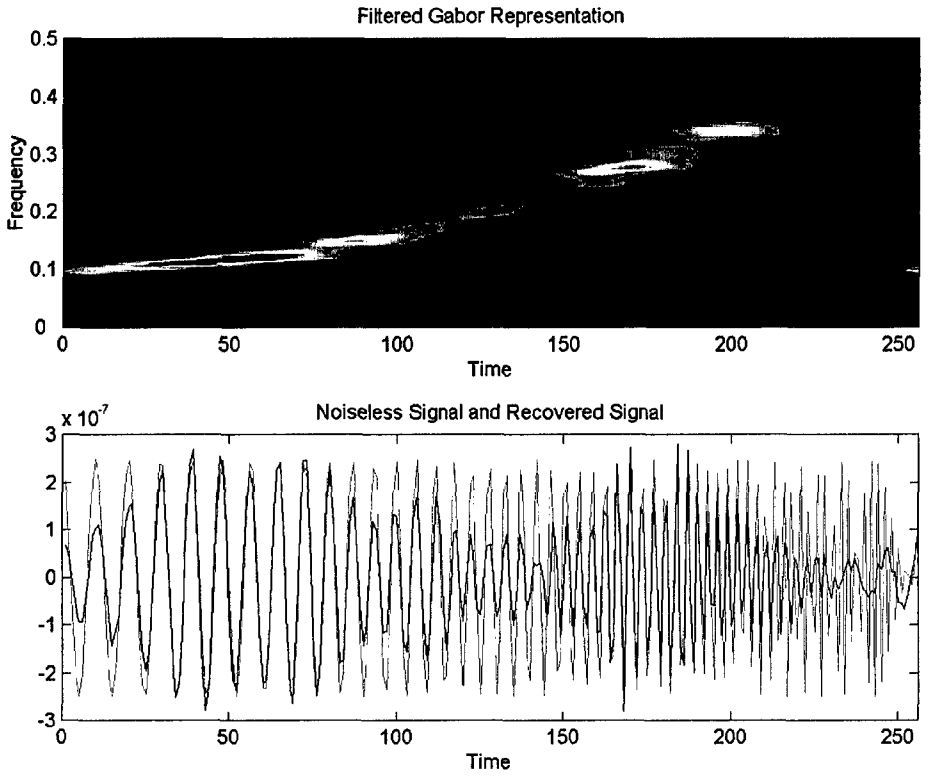

Figure 7: *Filtered time-frequency transform and time signals*

One of the applications of the time-frequency analysis is the detection of noise-corrupted signals. In general, random noise tends to spread evenly across the time and frequency domains. However, the signal usually concentrates in a relatively short period or a narrow frequency band. If one converts the noise-corrupted signal to the joint time-frequency domain, one can substantially improve the local or regional Signal-to-Noise (SNR).

2.3 Signal Analysis

This section will show the usefulness of time-frequency analysis in analyzing real aircraft data. The data had been collected by Pulse Doppler High Frequency Surface Wave Radar, which used a 10-element linear receiving antenna array. The data had been collected during the known presence of a target. The radar carrier frequency is 5.672 MHz and the pulse repetition frequency is 9.17762 Hz. The Fourier spectrum of this signal is shown in Figure 8. The central portion of the spectrum, which comprises two strong spectral spikes, is occupied by the sea-clutter. From the spectrum, it appears that the target is present between 0.3 and 0.4 Hz. The spread of its spectrum tells us very little about the target's behavior.

The time-frequency representation immediately provides more information. Figure 9 shows the Gabor representation of the signal. From Figure 9, the target signal can be seen increasing from slightly below 0.3 Hz to 0.4 Hz. The increase is non-uniform and occurs between time bins 150 and 225. This signifies that the target is accelerating moderately.

The original target signal can easily be recovered from the time-frequency representation. First the transform is filtered to obtain only the target signal. The filtered transform is then averaged over time to obtain the target signal in the frequency-domain. The frequency of the signal is then converted to the time-domain by an inverse Fourier transform. The filtered transform can be seen in Figure 10. The recovered signal compared to the original sampled data can be seen in Figure 11. The recovered signal is black and the original signal is grey.

Through the use of time-frequency representation, the analysis of the signal is greatly simplified. The image of the transform allows for quick, visual analysis of the target signal. Through the use of a filter, the original target signal can be easily recovered for further signature and detection analysis. When the SNR is very low, as with many radar signals, the joint time-frequency analysis might offer the only opportunity to detect the signal of interest.

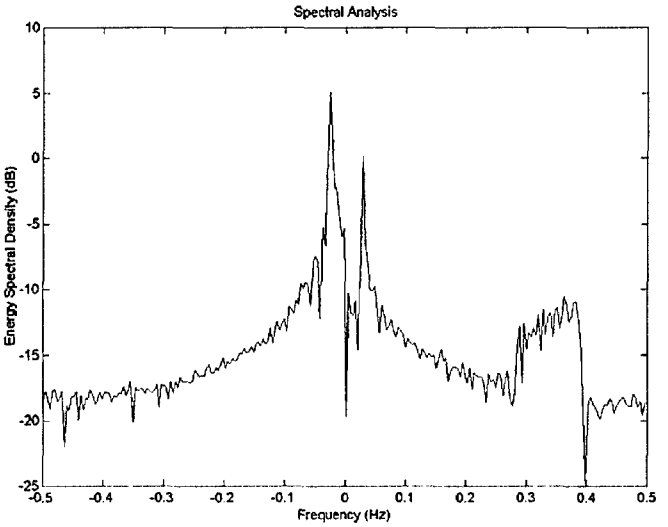

Figure 8: *Spectrum of noisy aircraft data*

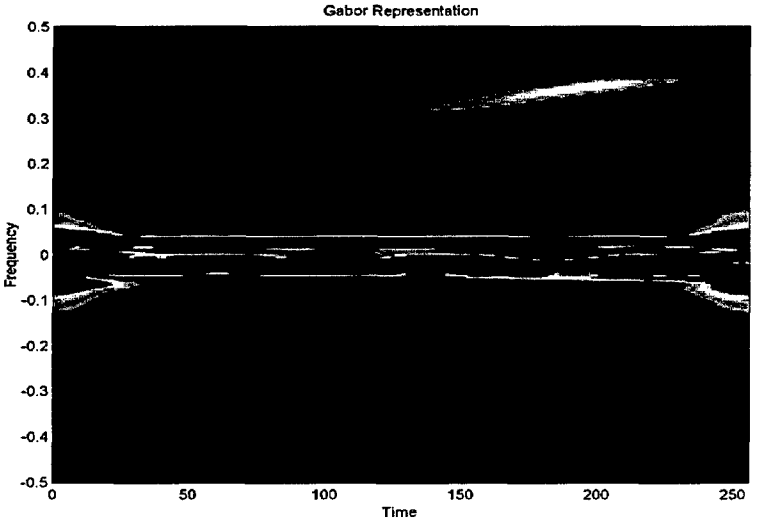

Figure 9: *The Gabor representation of the aircraft data*

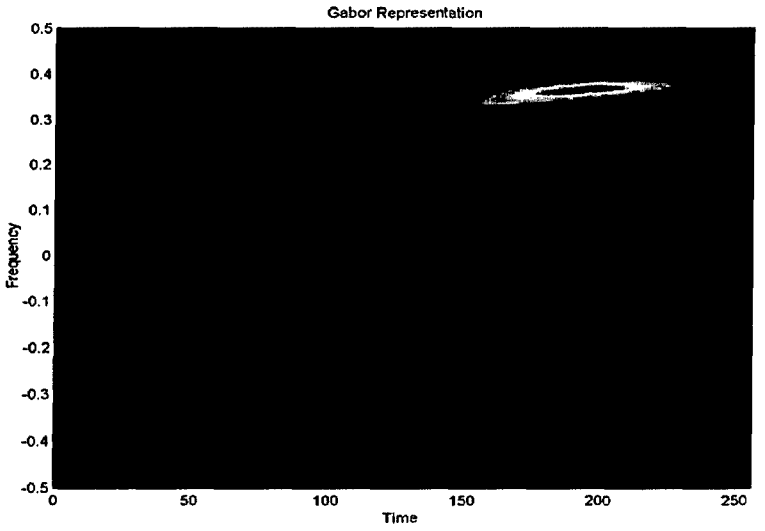

Figure 10: *Filtered Gabor representation*

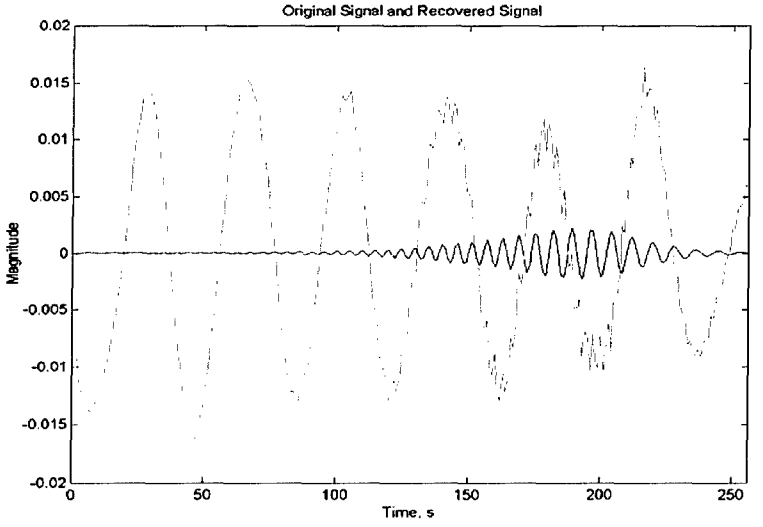

Figure 11: *Recovered target signal*

3. Comparison of Time-Frequency Distributions

There are many time-frequency distributions that have been developed. The transforms we will be examining include linear, bilinear, adaptive, and averaged transforms. All the time-frequency representations can be obtained from

$$C_x(t,\nu;f) = \int\int\int \exp^{j2\pi\xi(s-t)} f(\xi,\tau)x(s+\tau/2)x^*(s-\tau/2)\exp^{-j2\pi\nu\tau}\, d\xi ds d\tau \quad (1)$$

where x is the signal, t is the time, ν is the frequeny and τ is the running time. $f(\xi,\tau)$ is a two-dimensional function called the parameterization function or the kernel defined along the ξ-axis and τ-axis. This class of distribution is known as the Cohen's class [5-6,11-12], which can be written as

$$C_x(t,\nu;\Pi) = \int\int \Pi(s-t,\xi-\nu)W_x(s,\xi)ds d\xi \quad (2)$$

where

$$\Pi(t,\nu) = \int\int f(\xi,\tau)\exp^{-j2\pi(\nu\tau+\xi t)}\, dt d\nu \quad (3)$$

is a two-dimensional Fourier transform of the kernel function f and $W_x(s,\xi)$ is the Wigner-Ville distribution. This class is significantly important since it includes a large number of the existing time-frequency energy distributions. Moreover, this general class can be used to facilitate the design of new time-frequency transform. There are a number of alternative ways of writing the general class of time-frequency distributions that are convenient and add considerable physical insight into the process. The properties of a distribution are reflected by simple constraints on the kernel, by examining the kernel, one can readily ascertain the properties of the distribution. This allows one to pick and choose those kernels that produce distributions with prescribed, desirable properties. Moreover, the Wigner-Ville distribution is the element of the Cohen's class for which the function Π is a double Dirac: $\Pi(t,\nu) = \delta(t)\delta(\nu)$, i.e., $f(\xi,\tau) = 1$. For the Wigner-Ville distribution the kernel is one.

In this section we will begin with background information on the twelve transforms that are being evaluated. This background provides a short description of each time-frequency transform. Detailed descriptions, properties and derivations of the transforms can be found from the references, particularly from [5-7,12-14].

The performance of the twelve transforms will then be compared through five experimental radar data sets. These sets will range from returns with constant frequency to returns with non-uniform frequency modulation. Each transform will then be evaluated for its effectiveness in various situations.

3.1 Gabor Representation

The Gabor representation performs an expansion on a time signal. The expansion is represented as a finite set of time-shifted and frequency modulated signals. These signals are localized in a time-frequency plane. The Gabor expansion can be calculated with:

$$G_x[n,m;h] = \sum_{k=-\infty}^{\infty} x[k]h^*[k-n]\exp^{-2j\pi nk} \tag{4}$$

where x is the signal, h is the synthesis window, m is the number of Gabor coefficients in frequency and n is the number of Gabor coefficients in time. The Gabor representation is a linear time-frequency representation [15-16].

3.2 Margenau-Hill Spectrogram

The Margenau-Hill spectrogram is defined as:

$$MHS_x(t,\nu) = \Re\{K_{gh}^{-1}F_x(t,\nu;g)F_x^*(t,\nu;h)\} \tag{5}$$

where $K_{gh} = \int h(u)g^*(u)du$ and $F_x(t,\nu;g)$ is the short-time Fourier transform of x. h and g are the analysis windows. The Margenau-Hill spectrogram is a bilinear time-frequency representation [17-18].

3.3 Born-Jordan Distribution

The Born-Jordan distribution is a shift-invariant, kernel smoothed Wigner-Ville distribution. The kernel function defined for equation (3) is

$$f(\xi,\tau) = \frac{\sin(\pi\xi\tau)}{\pi\xi\tau} \tag{6}$$

which defines the Born-Jordan distribution as:

$$BJ_x(t,\nu) = \int_{-\infty}^{\infty} \frac{1}{|\tau|} \int_{t-|\tau|/2}^{t+|\tau|/2} x(s+\tau/2)x^*(s-\tau/2)ds.\exp^{-j2\pi\nu\tau}\, d\tau \tag{7}$$

where t is the time, ν is the frequency, x is the signal, and τ is the running time. The conjugation of x is x^*. The Born-Jordan distribution is a bilinear time-frequency representation [11].

3.4 Binomial Distribution

The binomial distribution is a shift-invariant, reduced interference distribution with a kernel based on the binomial coefficients. The binomial distribution is defined as:

$$RIBN_x(t,\nu) = \sum_{\tau=-\infty}^{\infty} \frac{1}{|\tau|} \sum_{\nu=-|\tau|}^{|\tau|} \frac{1}{2^{2|\tau|+1}} \begin{pmatrix} 2|\tau|+1 \\ |\tau+\nu+1| \end{pmatrix} x[t+\nu+\tau]x^*[t+\nu-\tau] \exp^{-j4\pi\nu\tau} \tag{8}$$

The binomial distribution is a bilinear time-frequency representation [19].

3.5 Choi-Williams Distribution

The Choi-Williams distribution was developed as a method of finding the Wigner-Ville distribution with the minimum amount of cross-term interference. The Choi-Williams distribution is a shift-invariant transform. Essentially, the distribution is a smoothed version of the Wigner-Ville distribution through a kernel function defined by

$$f(\xi,\tau) = \exp\left[-\frac{(\pi\xi\tau)^2}{2\sigma^2}\right] \tag{9}$$

The Choi-Williams distribution is then defined as

$$CW_x(t,\nu) = \sqrt{\frac{2}{\pi}} \int \int_{-\infty}^{\infty} \frac{\sigma}{|\tau|} \exp^{-2\sigma^2(s-t)^2/\tau^2} x(s+\frac{\tau}{2})x^*(s-\frac{\tau}{2}) \exp^{-j2\pi\nu\tau} \, ds d\tau \tag{10}$$

The smoothing of the distribution is controlled by the constant σ. As $\sigma \rightarrow \infty$, the Choi-Williams distribution will simplify converge to the Wigner-Ville distribution, as the kernel goes to 1. The cross-terms are reduced with smaller values of σ. The Choi-Williams distribution is a bilinear time-frequency representation [20].

3.6 Smoothed Wigner-Ville Distribution

The smoothed pseudo Wigner-Ville distribution is given as

$$SPWV_x(t,\nu;g,h) = \int_{-\infty}^{\infty} h(\tau) \int_{-\infty}^{\infty} g(s-t)x(s+\tau/2)x^*(s-\tau/2)ds \exp^{-j2\pi\nu\tau} \, d\tau \tag{11}$$

where h is the frequency smoothing window and g is the time smoothing window. The smoothed Wigner-Ville distribution considered in this analysis is Gaussian "smoothed". Smoothing the Wigner-Ville distribution causes a loss of phase information but it can eliminate to a certain degree the cross-term interference. The smoothed Wigner-Ville distribution is a bilinear time-frequency representation [13-14].

3.7 Spectrogram Distribution

The spectrogram distribution is the square of the short-time Fourier transform. It is also known as the energy density spectrum. An advantage of the spectrogram distribution is that it yields all positive values. The spectrogram is given as

$$SP_x(t,\nu) = \left| \int x(u) h^*(u-t) \exp^{-j2\pi\nu u} du \right|^2 \tag{12}$$

where h is the frequency smoothing window and h being normalized so as to be of unit energy. The spectrogram distribution is a bilinear time-frequency representation [6,13-14].

3.8 Zhao-Atlas-Marks Distribution

If we smooth the Born-Jordan distribution (section 3.3) along the frequency axis, we obtain the Zaao-Atlas-Marks distribution. The distribution is defined as

$$ZAM_x(t,\nu) = \int_{-\infty}^{\infty} \left[h(\tau) \int_{t-|\tau|/2}^{t+|\tau|/2} x(s+\tau/2) x^*(s-\tau/2) ds \right] \exp^{-j2\pi\nu\tau} d\tau \tag{13}$$

It is also known as the Cone-Shaped kernel distribution. The Zhao-Atlas-Marks distribution is a bilinear time-frequency distribution [21].

3.9 Reassigned Gabor Representation

The reassigned time-frequency representation performs an averaging method upon their base transform [13]. The average values are shifted to the center of gravity of the energy contributions. Through the averaging and shifting, bilinearity of the transform is lost. Time and frequency shift invariance is preserved and the energy reassignment obeys the conservation of energy requirement. The reassigned Gabor representation at point (t', ν') is given by the following expression

$$S_x^{(r)}(t', \nu'; h) = \int \int S_x(t,\nu;h) \delta(t' - \hat{t}(x;t,\nu)) \delta(\nu' - \hat{\nu}(x;t,\nu)) dt d\nu \tag{14}$$

where S_x is the spectrogram time-frequency distribution. The analysis window h used in this spectrogram is a Gassian window. The reassignment method moves each value of the spectrogram computed at any point (t, ν) to another point (t', ν'), which is the center of gravity of the signal energy distribution around (t, ν). $\hat{t}(x; t, \nu)$ and $\hat{\nu}(x; t, \nu)$ are defined as;

$$\hat{t}(x; t, \nu) = t - \Re\left\{\frac{F_x(t, \nu; T_h)F_x^*(t, \nu; h)}{|F_x(t, \nu; h)|^2}\right\} \tag{15}$$

and

$$\hat{\nu}(x; t, \nu) = \nu + \Im\left\{\frac{F_x(t, \nu; D_h)F_x^*(t, \nu; h)}{2\pi|F_x(t, \nu; h)|^2}\right\} \tag{16}$$

As well, $T_h(t) = t\,h(t)$ and $D_h(t) = \frac{dh}{dt}(t)$. The windows T_h and D_h defined above are colinear in this case.

3.10 Reassigned Morlet Scalogram

The Morlet scalogram is the square of the wavelet transform using Morlet wavelets [13]. The wavelet transform uses a windowing process different to the sliding window used in the short-time Fourier transform. The wavelet transform uses narrow windows at high frequencies and wide windows at low frequencies. The reassigned Morlet scalogram can be calculated as:

$$SC_x^{(r)}(t', a'; h) = \int\int a'^2 SC_x(t, a; h)\delta(t' - \hat{t}(x; t, a))\delta(a' - \hat{a}(x; t, a))\frac{dtda}{a^2} \tag{17}$$

where

$$\hat{t}(x; t, a) = t - \Re\left\{a\frac{T_x(t, a; T_h)T_x^*(t, a; h)}{|T_x(t, a; h)|^2}\right\} \tag{18}$$

and

$$\hat{\nu}(x; t, a) = \frac{\nu_0}{\hat{a}(x; t, a)} = \frac{\nu_0}{a} + \Im\left\{\frac{T_x(t, a; D_h)T_x^*(t, a; h)}{2\pi a|T_x(t, a; h)|^2}\right\} \tag{19}$$

with $T_h(t) = t\,h(t)$ and $D_h(t) = \frac{dh}{dt}(t)$, where $h(t)$ is a Gassian window. $SC_x(t, a; h)$ is the scalogram and $T_x(t, a; h)$ is the wavelet transform:

$$SC_x(t,a;h) = |T_x(t,a;h)|^2 = \frac{1}{|a|}\left|\int x(s)h^*(\frac{s-t}{a})ds\right|^2 \tag{20}$$

3.11 Reassigned Spectrogram Distribution

The reassigned spectrogram distribution performs an averaging and shifting method upon the spectrogram distribution [13]. The reassigned spectrogram is defined as:

$$S_x^{(r)}(t',\nu';h) = \int\int S_x(t,\nu;h)\delta(t'-\hat{t}(x;t,\nu))\delta(\nu'-\hat{\nu}(x;t,\nu))dtd\nu \tag{21}$$

where

$$\hat{t}(x;t,\nu) = t - \Re\left\{\frac{F_x(t,\nu;T_h)F_x^*(t,\nu;h)}{|F_x(t,\nu;h)|^2}\right\} \tag{22}$$

and

$$\hat{\nu}(x;t,\nu) = \nu + \Im\left\{\frac{F_x(t,\nu;D_h)F_x^*(t,\nu;h)}{2\pi|F_x(t,\nu;h)|^2}\right\} \tag{23}$$

$S_x(t,\nu;h)$ is the spectrogram distribution and $T_h(t) = t\,h(t)$ and $D_h(t) = \frac{dh}{dt}(t)$.

3.12 Adaptive Energy Distribution

Adaptive energy distribution (AED) is a window-matched spectrogram, in which the window matching is done with the use of generalized instantaneous parameters (GIP's). The GIP's that are used for Gaussian window matching are the instantaneous time variance (ITV), the instantaneous frequency variance (IFV), and the instantaneous time-frequency (ITF) covariance [22].

$$ITV_{zh}(t,\nu) = -\frac{1}{8\pi^2}\Re\left[\frac{\partial^2 S_x(t,\nu)}{\partial\nu^2}\frac{1}{S_x(t,\nu)} - \left(\frac{\partial S_x(t,\nu)}{\partial\nu}\frac{1}{S_x(t,\nu)}\right)^2\right] \tag{24}$$

$$IFV_{zh}(t,\nu) = -\frac{1}{8\pi^2}\Re\left[\frac{\partial^2 S_x(t,\nu)}{\partial t^2}\frac{1}{S_x(t,\nu)} - \left(\frac{\partial S_x(t,\nu)}{\partial t}\frac{1}{S_x(t,\nu)}\right)^2\right] \tag{25}$$

$$ITF_{zh}(t,\nu) = -\frac{1}{8\pi^2}\Re\left[\frac{\partial^2 S_x(t,\nu)}{\partial\nu\partial t}\frac{1}{S_x(t,\nu)} - \frac{\partial S_x(t,\nu)}{\partial\nu}\frac{\partial S_x(t,\nu)}{\partial t}\left(\frac{1}{S_x(t,\nu)}\right)^2\right] \tag{26}$$

where $S_x(t,\nu)$ specifies the spectrogram of the signal $x(t)$ formed using the window $h(t)$. The subscript zh in equations (24)-(26) denotes that the signal $x(t)$ has been multiplied by the window $h(t)$. The parameters for an optimal window are found by matching the GIP's of the signal-window spectrogram to those of the window-window spectrogram. The optimal window parameters are updated iteratively until the desired level of matching. At the n^{th} iteration they are calculated from

$$\alpha_{n+1}(t,\nu) = \frac{(8\pi)^3(ITF_{zh_n}(t,\nu))^2 IFV_{zh_n}(t,\nu)}{(8\pi)^2(ITF_{zh_n}(t,\nu))^2 + 1} \tag{27}$$

and

$$\beta_{n+1}(t,\nu) = \frac{(8\pi)^2 ITF_{zh_n}(t,\nu) IFV_{zh_n}(t,\nu)}{(8\pi)^2(ITF_{zh_n}(t,\nu))^2 + 1} \tag{28}$$

or if $ITV_{zh_n}(t,\nu) > IFV_{zh_n}(t,\nu)$ then

$$\alpha_{n+1}(t,\nu) = \frac{1}{8\pi \cdot ITV_{zh_n}(t,\nu)} \tag{29}$$

and

$$\beta_{n+1}(t,\nu) = \frac{1}{(8\pi)^2 ITV_{zh_n}(t,\nu) ITF_{zh_n}(t,\nu)} \tag{30}$$

where α and β are the parameters of the Gaussian window $h(t) = \exp^{-\pi(\alpha - j\beta)t^2}$.

4. Comparison of Transforms

4.1 Comparison Signals

The signals in the following comparisons are experimental aircraft data. These signals were collected by a High Frequency Pulse Doppler Surface Wave Radar, which used a 10-element linear receiving antenna array. The data was collected with a target present. The radar carrier frequency is 5.672 MHz and the pulse repetition frequency is 9.17762 Hz. There are 5 trials and each trial corresponds to a block of 256 pulses. The detailed description of the radar is given by [23,24].

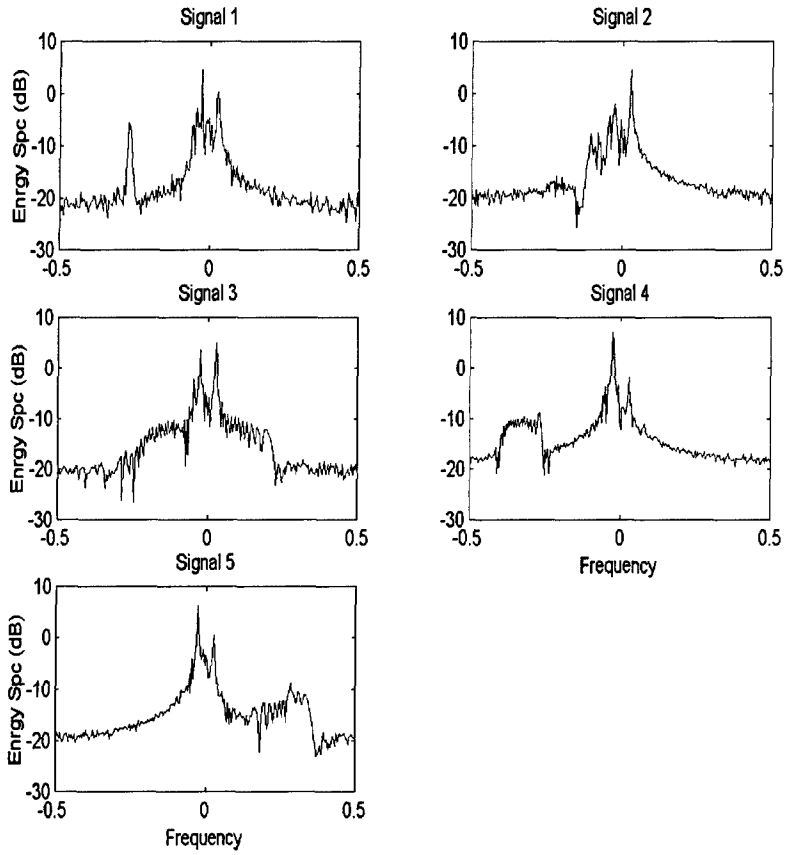

Figure 12: *Spectrums of the five comparison signals*

The Fourier spectrums of the five signals can be seen in Figure 12. In general, the background against which targets must be detected by a radar is clutter and noise (thermal and atmospheric). In the case of High Frequency Surface Wave Radar (HFSWR) used over the ocean, the clutter is due to Bragg scattering from the surface of

the ocean and is known as sea-clutter [23,24]. The sea-clutter components are concentrated around zero-Doppler with two large spectral spikes around zero-Doppler known as the Bragg lines. The spectral peak on the left hand side of Figure 12 is called the receding Bragg line. The one on the right hand side is called the advancing Bragg line. The Bragg lines appear as two very large targets. Nornally high speed aircraft appears in the flat portion of the Doppler spectrum. However, when the aircraft travels in a direction tangential to the radar beam, as in the cases of signals 2 and 3 in Figure 12, the aircraft target can appear in the velocity spectrum close to the zero value.

In Signal 1, the target is seen in the spectrum. The target is a spike at around –0.25 Hz. In Signal 2, the target is difficult to detect. It is near the clutter, but it is spread and difficult to distinguish from the clutter. In Signal 3, the target is spread widely from approximately –0.3 to 0.2 Hz. Whether the frequency has been increasing, decreasing, or oscillating is undeterminable. In Signal 4, the target is spread between –0.4 to –0.25 Hz. Whether the frequency has been increasing, decreasing, or oscillating is again undeterminable. In Signal 5, the target is spread from 0.35 Hz to the clutter. Whether the frequency has been increasing, decreasing, or oscillating is undeterminable.

These five signals were used to test the performance of 12 time-frequency transforms. The parameters, such as smoothing length or kernel spread, of each time-frequency representation were chosen to provide the best resolution of the target.

4.2 Constant Frequency

The first signal is a chirp with constant frequency modulation. This signal tests the ability of the transforms to resolve constant frequency modulation. The transforms are shown in Figure 13.

The target signal is perfectly resolved with the reassigned Gabor representation and the reassigned Morlet scalogram. The target signal is nearly perfectly resolved in time and frequency with all of the other transforms. Of these, the Choi-Williams distribution and the binomial distribution provide the sharpest response. The reassigned spectrogram's image of the target is very grainy. The adaptive energy distribution and the Zhao-Atlas-Marks distribution are slightly grainy when compared with the other transforms.

The smoothed Wigner-Ville distribution is the "noisiest" transform. The signal is very faint compared to the clutter and the interference cross-term. The Choi-Williams distribution is the second noisiest transform. While the interference cross-term is reduced, it is still quite visible. The binomial distribution and the Born-Jordan distribution have small smears between the signal and the clutter as the only remnants of the cross-term. The remaining transforms are relatively noiseless.

4.3 Non-Uniform Chirp near Clutter

The second signal is a chirp with non-uniform frequency modulation at normalized frequencies close to 0 Hz. This signal tests the ability of the transforms to detect a target signal close to the clutter. The transforms are shown in Figure 14.

The Born-Jordan distribution and the Zhao-Atlas-Marks distribution are unable to clearly display the signal close to the clutter. The target signal is broken up and joined with the clutter in various places.

The binomial distribution, the Choi-Williams distribution, and the smoothed Wigner-Ville distribution display the target signal, but it is nearly indistinguishable from the clutter.

The reassigned transforms provide perfect time and frequency resolution. The Gabor representation, the spectrogram, and the adaptive energy distribution provide nearly perfectly resolved signals in time and frequency, which are easily distinguishable from the clutter. The Margenau-Hill spectrogram provides very good frequency resolution, but its time resolution is not as good as the other transforms. The reassigned spectrogram and the adaptive energy distribution are grainy compared to the other transforms.

4.4 Chirp Through Clutter

The third signal contains a chirp with approximately linear frequency modulation. This chirp passes directly "through" the clutter. This signal tests the ability of the transform to resolve weak signals that pass through strong noisy clutter. The transforms are shown in Figure 15.

The target signal is visible within all of the transforms. With the Zhao-Atlas Marks distribution, the target is seen only as a disruption in the clutter. For the Born-Jordan distribution, the target signal is broken up and smeared with the clutter.

The reassigned Gabor representation and the reassigned Morlet scalogram perfectly resolve the target signal in time and frequency. The clutter has minimal effect on displaying the target signal. The smoothed Wigner-Ville, the binomial distribution, the Choi-Williams distribution, and the reassigned spectrogram also provide excellent signal resolution in time and frequency. The cross-term interference is significant with the binomial distribution, Choi-Williams distribution and the smoothed Wigner-Ville distribution. Some parts of the target signal have been slightly masked by the interference. The remaining transforms provide decent frequency resolution. The target is smeared in the frequency-domain for these transforms, but it is visible and does not suffer from interference. The Gabor representation and the spectrogram distribution provide the best image of the target signal of these remaining transforms.

4.5 Changing Signal

The fourth signal is a chirp that changes from a linear frequency modulation to a constant modulation. This signal tests the ability to display a target signal that changes its characteristic behavior. The transforms are shown in Figure 16.

The target return is perfectly resolved in time and frequency with the reassigned Gabor representation and the reassigned Morlet scalogram. The constant portion of the signal is faint, but is still visible for both transforms. The smoothed Wigner-Ville distribution, the binomial distribution, the Choi-Williams distribution and the reassigned spectrogram distribution provide a nearly perfectly resolved target signal in time and frequency. The constant portion of the signal is faint with the reassigned spectrogram. The Choi- Williams distribution and the smoothed Wigner-Ville distribution have significant cross-term interference. The binomial distribution has a small cross-term remaining.

The Zhao-Atlas-Marks distribution does not resolve the target clearly. The target is smeared and grainy. The clutter with this distribution appears much larger than with the other distributions.

The remaining transforms are a mix of decent and good resolution. For the linear frequency modulation, the target signal is well resolved in time and frequency. The constant portion is much sharper. The Gabor representation, the Margenau-Hill spectrogram and the adaptive energy distribution provide the best images of the target of these remaining transforms. The Born-Jordan distribution has cross-term interference approximately equal in magnitude to the target signal.

4.6 Small Frequency Modulation

The final signal contains a target signal with nearly linear frequency modulation. The modulation begins by increasing non-uniformly. It then remains constant for a period, and then increases again. This signal tests the ability to detect minor changes in the behavior of a signal. The transforms are shown in Figure 17.

The reassigned Gabor representation and the reassigned Morlet scalogram display a perfectly resolved target signal in both time and frequency. All three portions of the target signal are clearly visible. The smoothed Wigner-Ville, the binomial, and the Choi-Williams distributions provide nearly perfectly resolved target signals in time and frequency. A strong interference cross-term is present with the smoothed Wigner-Ville distribution. A smeared cross-term is still visible with the binomial distribution. A strong, smeared cross-term is visible with the Choi-Williams distribution. These distributions show the three portions of the signal clearly.

The Zhao-Atlas-Marks distribution displays a grainy target with poor frequency resolution. The clutter appears strongest with this transform.

The remaining transforms provide similar resolution of the target signal. While the three portions of the signal are visible in all of the transforms, certain transforms do not display them very well. The curves of the target signal are less pronounced with the Gabor representation, the Margenau-Hill spectrogram, and the adaptive energy distribution, which make the target return appear to be a linear chirp. The Born-Jordan distribution displays the nature of the signal well, but it is grainy and smeared along the frequency axis. The spectrogram and the reassigned spectrogram provide good time and frequency resolution, but the reassigned spectrogram is very grainy.

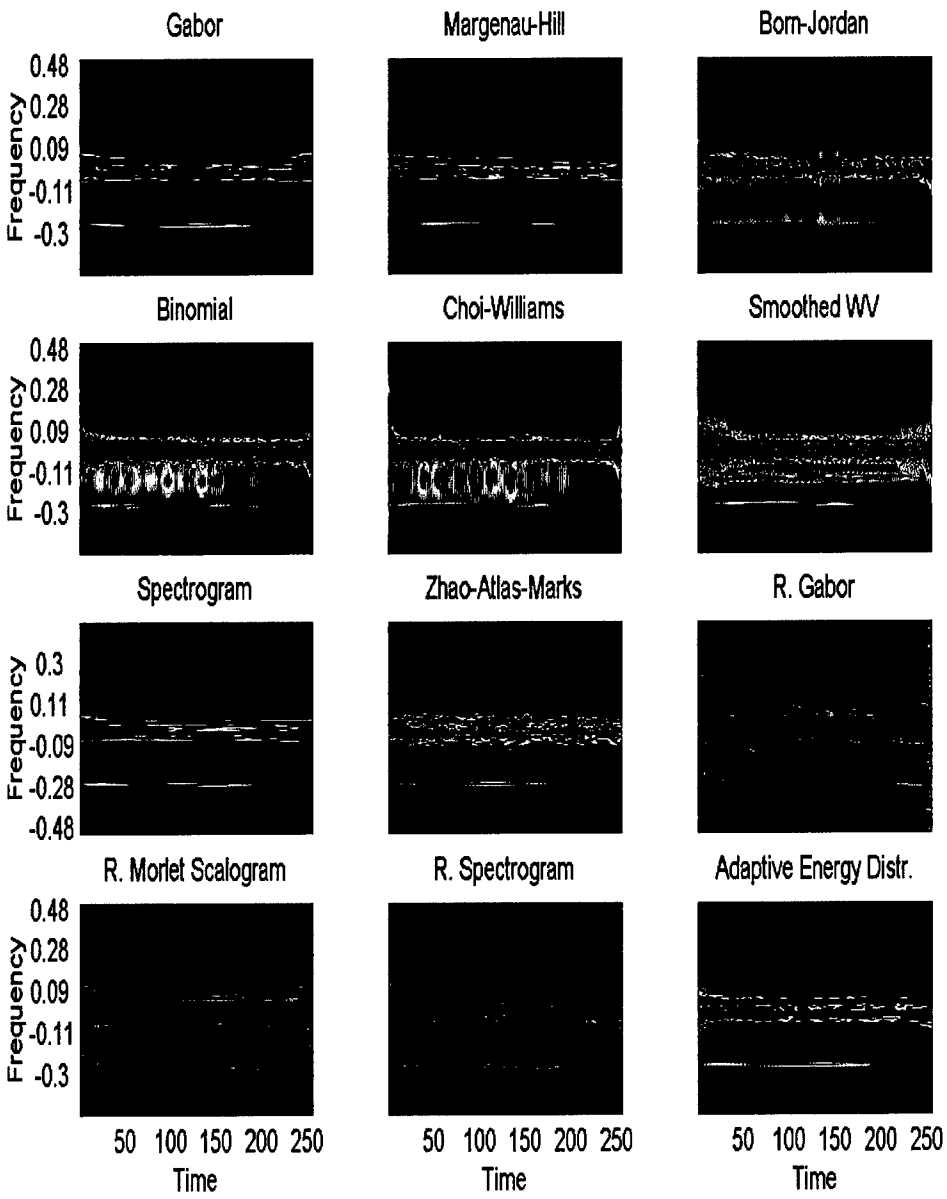

Figure 13: *Time-frequency representations of a signal with constant frequency.*

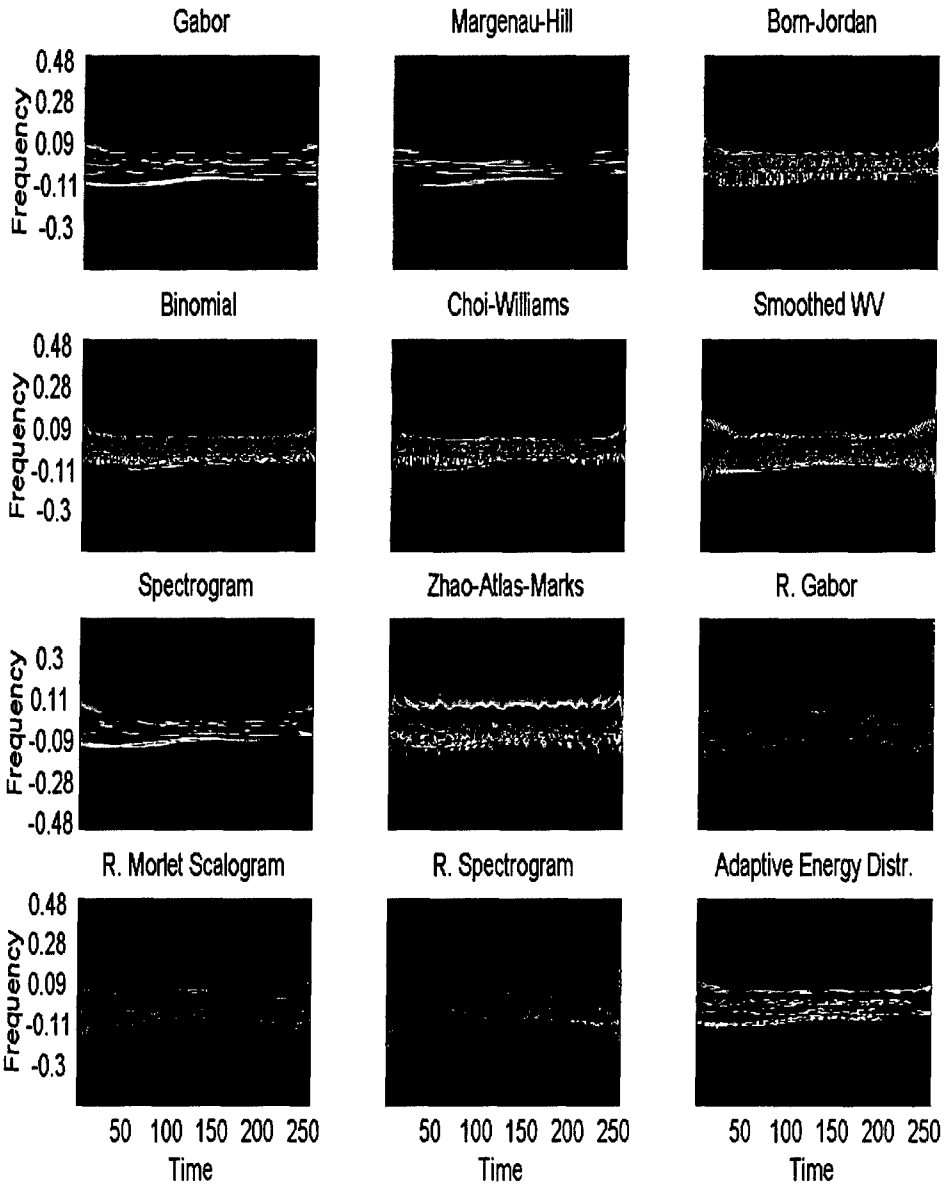

Figure 14: *Time-frequency representations of a signal near clutter.*

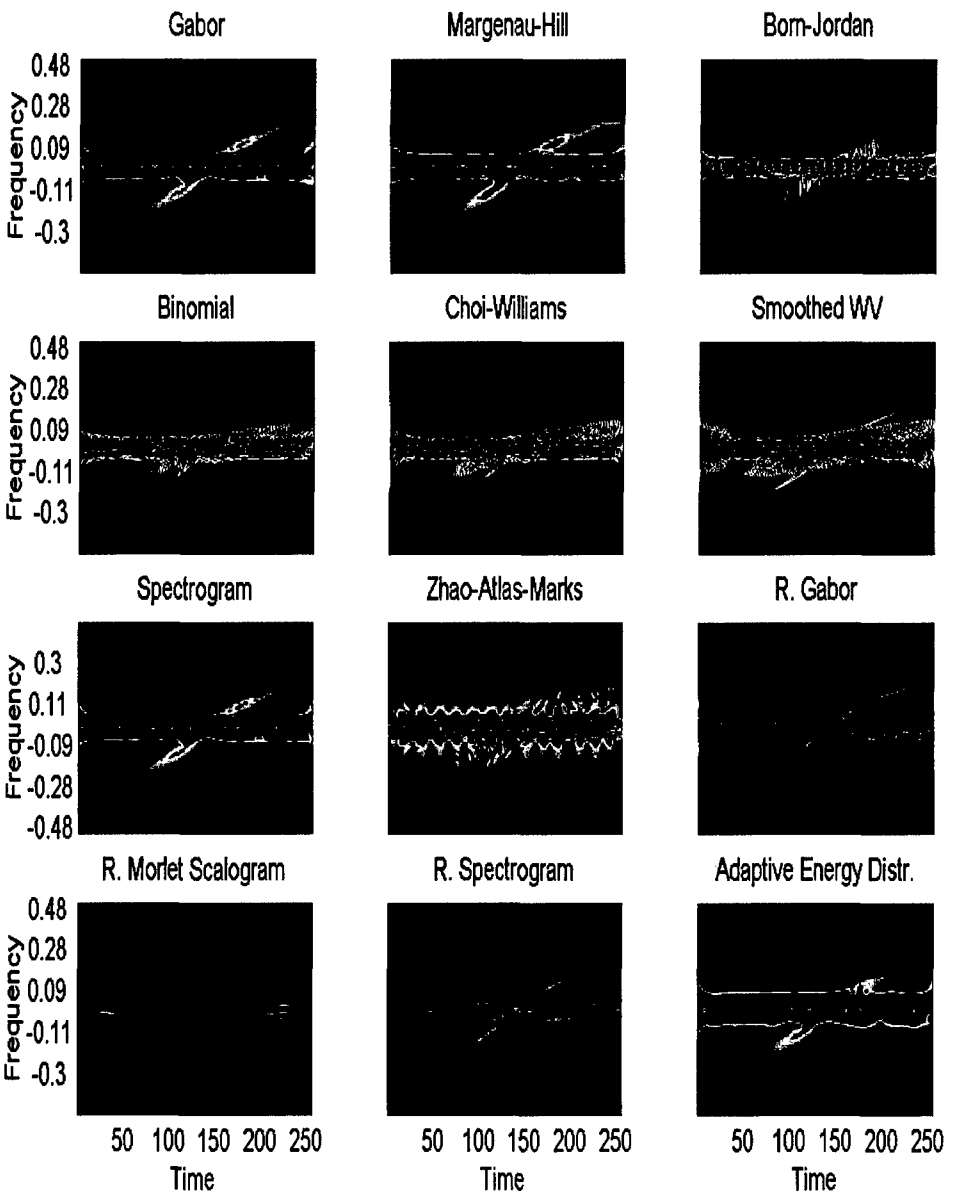

Figure 15: *Time-frequency representations of a signal through clutter.*

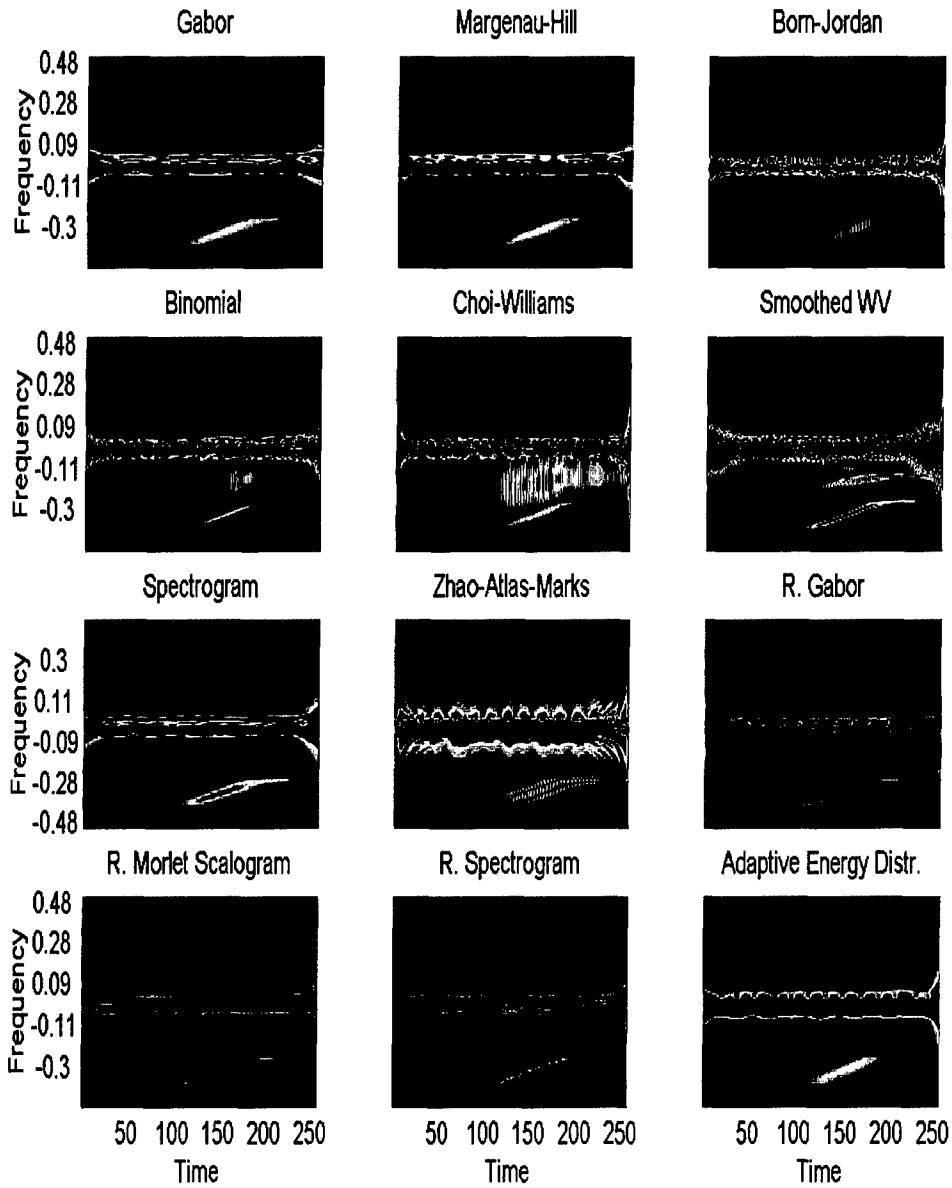

Figure 16: *Time-frequency representations of the changing signal.*

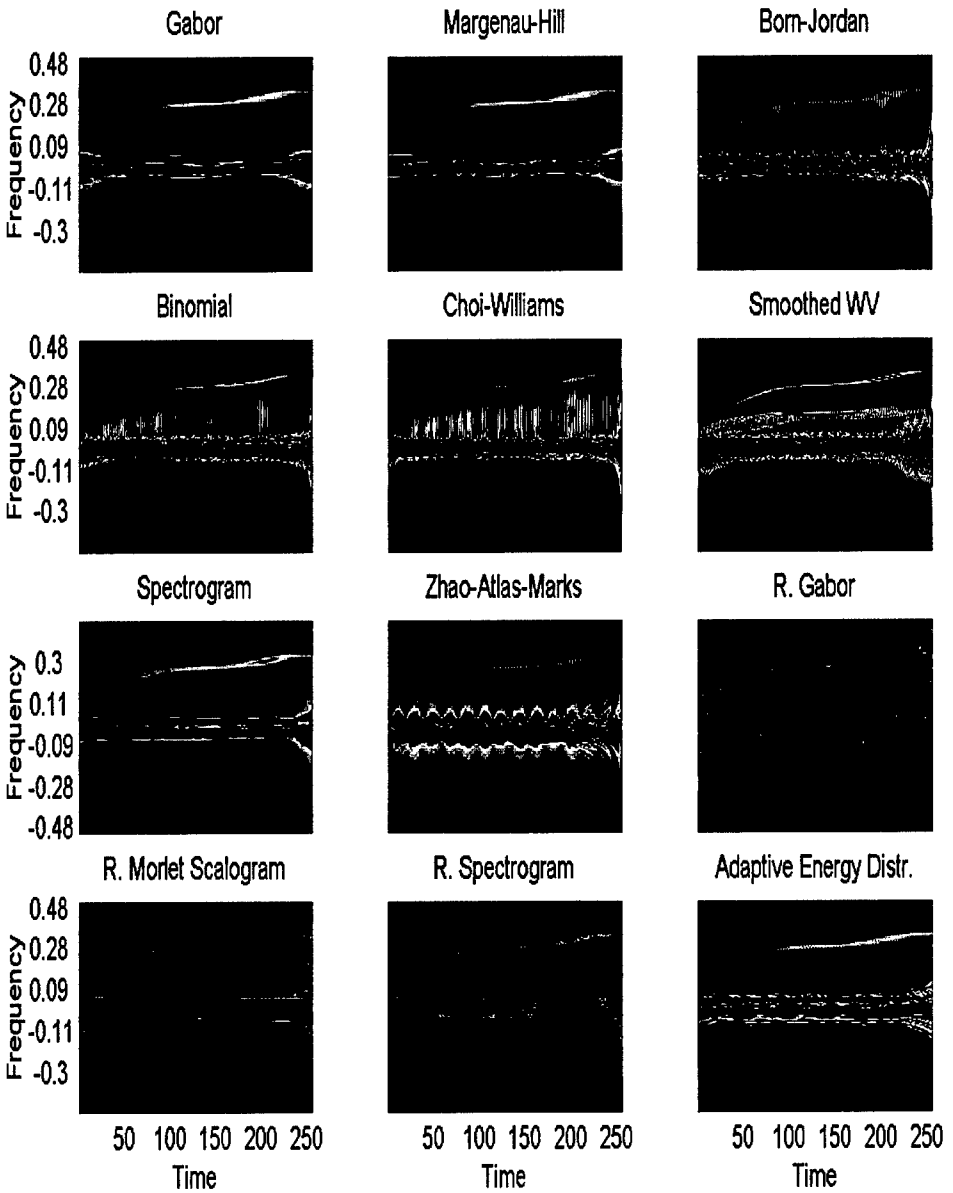

Figure 17: *Time-frequency representation of a signal with small frequency modulation.*

5. Evaluation of Transforms

5.1 Gabor Representation

The Gabor representation provides excellent resolution in time and frequency for all signals except those with a large chirp. Signals close to the clutter are not affected by the clutter. No cross-term interference is present in the Gabor representation. The Gabor representation has difficulty in sharply resolving chirp signals. The signal is smeared for large frequency changes. For cases where frequency changes are small, the Gabor representation is a good transform.

5.2 Margenau-Hill Spectrogram

The Margenau-Hill spectrogram provides good resolution in time and frequency for all signals except the chirp through the clutter. For signals close to the clutter, the transform loose some time resolution. This transform has no cross-term interference. For cases where frequency changes are small, the Margenau-Hill spectrogram is a good transform.

5.3 Born-Jordan Distribution

The Born-Jordan distribution performs well for signals with constant frequency. The signal is warped and broken up for signals close to the clutter. The distribution displays smeared cross-term interference, although it is generally weaker than the signal. For signals with frequency modulation, the Born-Jordan distribution does not provide a smooth target image. This transform is not ideal due to its inability to resolve targets near clutter and its poor resolution with chirp signals.

5.4 Binomial Distribution

The binomial distribution provides good resolution in time and frequency for signals of all types. The signal is still visible close to clutter, although cross-term interference impedes easy signal detection. Smeared cross-term interference is present in the binomial distribution. Its magnitude ranges from weaker than the signal to stronger than the signal depending on the proximity of the signal to the clutter. For cases where the cross-term interference is not important and the target is not close to the clutter, the binomial distribution is a good transform.

5.5 Choi-Williams Distribution

The Choi-Williams distribution provides excellent resolution in time and frequency for signals of all types. Signals close to clutter are difficult to detect due to interference. Smeared cross-term interference is present in the Choi-Williams distribution, with a magnitude ranging from slightly less to greater than the magnitude of the signal. For

cases where the cross-term interference is not important and the target is not close to the clutter, the Choi-Williams distribution is a good transform.

5.6 Smoothed Wigner-Ville Distribution

The smoothed Wigner-Ville distribution provides excellent time and frequency resolution in all cases. Signals close to the clutter are visible but cross-term interference makes detection difficult. The cross-term interference is prominent in all signals, with large cross-terms with magnitudes greater than the signal. For signals that are not close to the clutter and cross-terms are not important, the smoothed Wigner-Ville distribution is an excellent transform.

5.7 Spectrogram Distribution

The spectrogram distribution provides good resolution in cases of constant frequency and small frequency changes. Signals close to the clutter show no interference. There is no cross-term interference present in this transform. For signals that have small frequency changes, the spectrogram distribution is a good transform.

5.8 Zhao-Atlas-Marks Distribution

The Zhao-Atlas-Marks distribution provides good resolution in the case of a constant frequency. Signals close to the clutter are broken up and combined with the clutter in some places. Smeared cross-term interference is visible with this transform. For signals with changing frequency, the Zhao-Atlas-Marks distribution displays ghosting around the signal. The ghosting increases when the rate of frequency change increases. The Zhao-Atlas-Marks is not an ideal transform due to its poor performance with signals close to the clutter and signals with changing frequency.

5.9 Reassigned Gabor Representation

The reassigned Gabor representation provides excellent time and frequency resolution in all cases. The signal crossing the clutter is not affected by the clutter. Signals close to the clutter are broken up and joined with the clutter in some places. There is no cross-term interference in this transform. For signals that are not close to the clutter, the reassigned Gabor representation is an excellent transform.

5.10 Reassigned Morlet Scalogram

The reassigned Morlet scalogram provides excellent time and frequency resolution in all cases. Signals close to the clutter are not affected by the clutter. There is no cross-term interference in this transform. The reassigned Morlet scalogram is an excellent transform.

5.11 Reassigned Spectrogram Distribution

The reassigned spectrogram distribution provides very good time and frequency resolution in all cases. Signals close to the clutter are not affected by the clutter. There is no cross-term interference in this transform. The image produced by the reassigned spectrogram distribution is not smooth. The reassigned spectrogram distribution is a very good transform.

5.12 Adaptive Energy Distribution

The adaptive energy distribution performs quite well for signals with constant frequency and small frequency changes. It avoids interference when the target signal is close to or passing through clutter. The adaptive energy distribution also does not display any cross-term interference. The transform has poor frequency resolution for signals with larger frequency changes. For cases with small or no frequency modulation, the adaptive energy distribution is a good transform.

6. Overall Evaluation

For the best possible resolution, the reassigned transforms should be used. The averaging algorithm guarantees signals perfectly localized in frequency. The only downside to these transforms is the time involved for their calculation. Before reassignment, the base transform must be performed. The reassignment can increase the total time for calculation by a factor of two or more.

In cases where resolution is not the main concern, the Gabor representation, the Margenau-Hill spectrogram, and the spectrogram distribution are good transforms to use. They are relatively quick compared to the other transforms. While they do not provide great resolution in cases of large frequency modulation, they accurately display the signal.

The binomial distribution, the Choi-Williams distribution, and the smoothed Wigner-Ville distribution provide very good resolution and good speed at the expense of some interference cross-terms. For target signals away from the clutter, the target and the cross-term are easy to identify. If the target is close to the clutter, the cross-terms make detection of the signal difficult.

7. Conclusion

Joint time-frequency representations provide excellent ways of analyzing non-stationary signals. Their ability to display frequencies that change in time is an improvement over Fourier analysis of signals. This study also shows that time-frequency transforms provide additional insight into the analysis, interpretation, and processing of radar signals that are sometimes superior to what is achievable in the traditional time or frequency domain alone.

With the Fourier spectrum, multi-component signals were difficult to detect, much less analyze. With time-frequency representations, the components of a signal were immediately visible due to the ability to show time-varying frequency.

Noise in signals greatly hampered the Fourier spectrum's ability to detect and analyze signals. While noise affected target detection with the time-frequency analysis, its effect was much less. The noise could be filtered out relatively easily, which allowed for the recovery of the target signal.

The ability of time-frequency analysis to analyze signals is demonstrated using a real signal from HF radar. The process from identification to recovery of the target signal was shown.

Several time-frequency transforms have been compared and evaluated using experimental HF radar data for detecting maneuvering air targets in sea-clutter environment. Each set of data tested the ability of the transforms to resolve different types of signals. While each transform had their own strengths and weaknesses, several transforms stood out for their flexibility and target image resolution.

From the data used in this report, the reassigned transforms provided the best signal resolution at the expense of computational time. The Gabor representation, the Margenau-Hill spectrogram and spectrogram distribution provided a quick alternative for simple analysis at the expense of resolution. The binomial distribution, the Choi-Williams distribution, and the smoothed Wigner-Ville provided a good balance of speed and resolution at the expense of some cross-term interference. These results demonstrated that joint time-frequency analysis techniques provide an effective method of detecting maneuvering air targets in heavily cluttered regions.

References

1. Hubbard, B. B. (1998). The world according to wavelets, Second edition, A. K. Peters, Wellesley, Massachusetts.

2. Qian, S. (2002). Time-frequency and wavelet transforms, *Prentice-Hall Inc.*, New York, USA

3. Yasotharan, T. and Thayaparan, T. (2002). Strengths and Limitation of the Fourier method for detecting accelerating targets by pulse Doppler radar, *IEE Proceedings - Radar Sonar Navig.*, vol. 149, pp. 83-88.

4. Thayaparan, T. (2000). Limitation and Strengths of the Fourier transform method to detect accelerating targets, *Defence R & D Canada*, DREO TM 2000-078.

5. Cohen, L. (1989). Time-Frequency Distributions - A Review, *Proc. IEEE,* vol. 77, pp. 941-981 1989.

6. Cohen, L. (1995). Time-frequency analysis, *Prentice-Hall Inc.*, New York, USA.

7. Hlawatsch, F. and Boudreaux-Bartels, G.F., Linear and Quadratic Time- Frequency Signal Representations, *IEEE Signal Processing Magazine*, April, 1992.

8. Chen, V. C. and Ling, H. (2002). Time-Frequency Transforms for Radar Imagine and Signal Analysis, *Artech House*, Boston, MA, USA.

9. Qian, S. and Chen, D. (1996). Joint time-frequency analysis: methods and applications, *Prentice-Hall Inc.*, New York, USA.

10. Thayaparan, T. (2000). Linear and quadratic time-frequency representations, *Defence R & D Canada*, DREO TM 2000-080.

11. Cohen, L. (1966). Generalized phase-space distribution functions, *J. Math. Phys.*, vol. 7. pp. 781-786.

12. Claasen, T. A. C. M. and Mecklenbräuker, W. F. G. (1980). The Wigner distribution - a tool for time-frequency signal analysis - part III: Relations with other time-frequency signal transformation, *Philips Jour. Research.*, vol. 35, pp. 372-389.

13. Auger, F. and Flandrin, P. (1995). Improving the readability of time-frequency and time-scale representations by the reassignment method, *IEEE Transactions on Signal Processing*, vol. 43, pp. 1068-1089.

14. Auger, F., Flandrin, P., Gonçalvès, P. and Lemoine, O. (1995). Time-frequency toolbox tutorial, *Rice University*, USA.

15. Zibulski, Z. (1993). Oversampling in the Gabor scheme, *IEEE on Signal Processing*, vol. 41, pp. 2679-87.

16. Wexler, R. (1990). Discrete Gabor transform, *Signal Processing*, vol. 21, pp. 207-221.

17. Margenhau, H. and Hill, R. (1961). Correlation between measurements in quantum theory, *Prog. Theor. Phys.*, vol. 26, pp. 722-738.

18. Hippentiel, R. and De Oliviera, P. (1990). Time-varying spectral estimation using the instantaneous power spectrum (IPS), *IEEE Trans. on Acoust.*, vol. 38, pp. 1752-1759.

19. Williams, W. and Jeong, J. (1992). Reduced interference time-frequency distributions in time-frequency analysis - methods and applications edited by B. Boashash, *Longman-Cheshire*, Melbourne.

20. Choi, H. and Williams, W. (1989). Improved time-frequency representation of multicomponent signals using exponential kernels, *IEEE Trans. on Acoustics, Speech and Signal Processing*, vol. 37, pp. 862-871.

21. Zhao, Y., Atlas, L. and Marks, R. (1990). The use of the cone-shaped kernels for generalized time-frequency representations of nonstationary signals, *IEEE Trans. on Acoustics, Speech and Signal Processing*, vol. 38, pp. 1084-1091.

22. Jones, G. and Boashash, B. (1997). Generalized instantaneous parameters and window matching in the time-frequency plane, *IEEE Transactions on Signal Processing*, vol. 45, pp. 1264-1275.

23. Chan, H. C. (1997). Iceberg detection and tracking using high frequency surface wave radar, *Defence R & D Canada*, DREO TR-1310.

24. Chan, H. C. (1998). Detection and tracking of low-altitude aircraft using HF surface-wave radar, *Defence R & D Canada*, DREO TR-1334.

DOCUMENT CONTROL DATA

(Security classification of title, body of abstract and indexing annotation must be entered when the overall document is classified)

1. ORIGINATOR (the name and address of the organization preparing the document. Organizations for whom the document was prepared, e.g. Establishment sponsoring a contractor's report, or tasking agency, are entered in section 8.)

Defence R&D Canada - Ottawa
Ottawa, Ontario, Canada K1A 0Z4

2. SECURITY CLASSIFICATION (overall security classification of the document, including special warning terms if applicable)

UNCLASSIFIED

3. TITLE (the complete document title as indicated on the title page. Its classification should be indicated by the appropriate abbreviation (S,C or U) in parentheses after the title.)

APPLICATION OF JOINT TIME-FREQUENCY REPRESENTATIONS TO A MANEUVERING AIR TARGET IN SEA-CLUTTER: ANALYSIS BEYOND FFT (U)

4. AUTHORS (Last name, first name, middle initial)

Thayaparan, Thayananthan; Kennedy, Steven

5. DATE OF PUBLICATION (month and year of publication of document)	6a. NO. OF PAGES (total containing information. Include Annexes, Appendices, etc.)	6b. NO. OF REFS (total cited in document)
March 2003	46	24

7. DESCRIPTIVE NOTES (the category of the document, e.g. technical report, technical note or memorandum. If appropriate, enter the type of report, e.g. interim, progress, summary, annual or final. Give the inclusive dates when a specific reporting period is covered.)

DRDC Ottawa TECHNICAL MEMORANDOM

8. SPONSORING ACTIVITY (the name of the department project office or laboratory sponsoring the research and development. Include the address.)

Defence R&D Canada - Ottawa
Ottawa, Ontario, Canada K1A 0Z4

9a. PROJECT OR GRANT NO. (if appropriate, the applicable research and development project or grant number under which the document was written. Please specify whether project or grant)	9b. CONTRACT NO. (if appropriate, the applicable number under which the document was written)
11ar15	

10a. ORIGINATOR'S DOCUMENT NUMBER (the official document number by which the document is identified by the originating activity. This number must be unique to this document.)	10b. OTHER DOCUMENT NOS. (Any other numbers which may be assigned this document either by the originator or by the sponsor)
DRDC Ottawa TM 2003-090	

11. DOCUMENT AVAILABILITY (any limitations on further dissemination of the document, other than those imposed by security classification)

(X) Unlimited distribution
( ) Distribution limited to defence departments and defence contractors; further distribution only as approved
( ) Distribution limited to defence departments and Canadian defence contractors; further distribution only as approved
( ) Distribution limited to government departments and agencies; further distribution only as approved
( ) Distribution limited to defence departments; further distribution only as approved
( ) Other (please specify):

12. DOCUMENT ANNOUNCEMENT (any limitation to the bibliographic announcement of this document. This will normally correspond to the Document Availability (11). However, where further distribution (beyond the audience specified in 11) is possible, a wider announcement audience may be selected.)

13. ABSTRACT (a brief and factual summary of the document. It may also appear elsewhere in the body of the document itself. It is highly desirable that the abstract of classified documents be unclassified. Each paragraph of the abstract shall begin with an indication of the security classification of the information in the paragraph (unless the document itself is unclassified) represented as (S), (C), or (U). It is not necessary to include here abstracts in both official languages unless the text is bilingual).

(U) Traditionally, radar signals have been analysed in either the time or the frequency domain. Joint time-frequency representations characterize signals over a time-frequency plane. They thus combine time-domain and frequency-domain analyses to yield a potentially more revealing picture of the temporal localization of a signal's spectral components. Therefore, for signals with time-varying frequency contents, the joint time-frequency representations offer a powerful analysis tool. A concise review of time-frequency transforms is provided as background needed to appreciate how time-frequency processing methods can improve conventional time or frequency processing methods. The report then describes and illustrates the advantages of using joint time-frequency techniques to analyze a multi-component signal, a noisy signal, and experimental aircraft data. Finally, we use time-frequency analysis techniques for the detection of maneuvering aircraft using HF radar in heavily cluttered regions. We compare the ability of different time-frequency transforms to resolve several experimental aircraft signals. The results clearly demonstrate that time-frequency analysis techniques can significantly improve the detection performance of the HF radar and add considerable physical insight over what can be achieved by conventional Fourier transform methods currently used by HF radars.

14. KEYWORDS, DESCRIPTORS or IDENTIFIERS (technically meaningful terms or short phrases that characterize a document and could be helpful in cataloguing the document. They should be selected so that no security classification is required. Identifiers such as equipment model designation, trade name, military project code name, geographic location may also be included. If possible keywords should be selected from a published thesaurus. e.g. Thesaurus of Engineering and Scientific Terms (TEST) and that thesaurus-identified. If it is not possible to select indexing terms which are Unclassified, the classification of each should be indicated as with the title.)

Time-Frequency Distribution
High Frequency Surface Wave Radar
Fourier Transform
Doppler Smearing
Sea-Clutter
Gabor Representation
Signal-to-Noise ratio
Spectrogram
Wigner Ville Distribution
Reassigned Spectrogram
Adaptive Energy Distribution
Wavelet transform
Detection